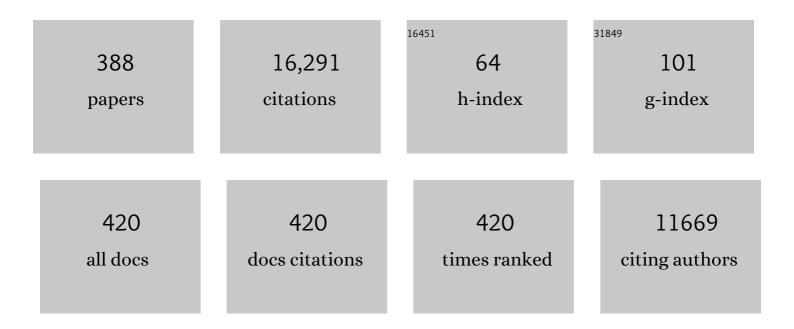
List of Publications by Year in descending order

Source: https://exaly.com/author-pdf/7674577/publications.pdf Version: 2024-02-01



#	Article	IF	CITATIONS
1	Surface-enhanced resonance Raman spectroscopy of Rhodamine 6G adsorbed on colloidal silver. The Journal of Physical Chemistry, 1984, 88, 5935-5944.	2.9	1,394
2	Electron-Transfer Processes of Cytochrome c at Interfaces. New Insights by Surface-Enhanced Resonance Raman Spectroscopy. Accounts of Chemical Research, 2004, 37, 854-861.	15.6	236
3	Spectroscopic Characterization of Nonnative Conformational States of Cytochrome c. Journal of Physical Chemistry B, 2002, 106, 6566-6580.	2.6	234
4	Role of water in bacteriorhodopsin's chromophore: resonance Raman study. Biochemistry, 1984, 23, 5539-5548.	2.5	228
5	Cytochrome c at charged interfaces. 1. Conformational and redox equilibria at the electrode/electrolyte interface probed by surface-enhanced resonance Raman spectroscopy. Biochemistry, 1989, 28, 6710-6721.	2.5	183
6	Heterogeneous Electron Transfer of Cytochrome c on Coated Silver Electrodes. Electric Field Effects on Structure and Redox Potential. Journal of Physical Chemistry B, 2001, 105, 1578-1586.	2.6	180
7	Proton-Coupled Electron Transfer of Cytochromec. Journal of the American Chemical Society, 2001, 123, 4062-4068.	13.7	180
8	Mutational Analysis of Deinococcus radiodurans Bacteriophytochrome Reveals Key Amino Acids Necessary for the Photochromicity and Proton Exchange Cycle of Phytochromes. Journal of Biological Chemistry, 2008, 283, 12212-12226.	3.4	180
9	Copper incorporation into recombinant CotA laccase from Bacillus subtilis: characterization of fully copper loaded enzymes. Journal of Biological Inorganic Chemistry, 2008, 13, 183-193.	2.6	173
10	Phenoxyl Radical Complexes of Zinc(II). Journal of the American Chemical Society, 1997, 119, 8889-8900.	13.7	167
11	Light-induced Proton Release of Phytochrome Is Coupled to the Transient Deprotonation of the Tetrapyrrole Chromophore. Journal of Biological Chemistry, 2005, 280, 34358-34364.	3.4	149
12	Protonation State and Structural Changes of the Tetrapyrrole Chromophore during the Pr→ PfrPhototransformation of Phytochrome: A Resonance Raman Spectroscopic Studyâ€. Biochemistry, 1999, 38, 15185-15192.	2.5	141
13	Redox and redox-coupled processes of heme proteins and enzymes at electrochemical interfaces. Physical Chemistry Chemical Physics, 2005, 7, 3773.	2.8	141
14	Alkaline Conformational Transitions of FerricytochromecStudied by Resonance Raman Spectroscopy. Journal of the American Chemical Society, 1998, 120, 11246-11255.	13.7	140
15	Disentangling interfacial redox processes of proteins by SERR spectroscopy. Chemical Society Reviews, 2008, 37, 937.	38.1	139
16	Surface-enhanced resonance Raman spectroscopy of cytochrome c at room and low temperatures. The Journal of Physical Chemistry, 1986, 90, 6017-6024.	2.9	126
17	Lewis Acid Trapping of an Elusive Copper–Tosylnitrene Intermediate Using Scandium Triflate. Journal of the American Chemical Society, 2012, 134, 14710-14713.	13.7	120
18	Tyrosine hydrogen-bonding and environmental effects in proteins probed by ultraviolet resonance Raman spectroscopy. Biochemistry, 1988, 27, 5426-5433.	2.5	114

#	Article	IF	CITATIONS
19	Phenoxyl-copper(II) complexes: models for the active site of galactose oxidase. Journal of Biological Inorganic Chemistry, 1997, 2, 444-453.	2.6	114
20	In Situ Spectroelectrochemical Investigation of Electrocatalytic Microbial Biofilms by Surfaceâ€Enhanced Resonance Raman Spectroscopy. Angewandte Chemie - International Edition, 2011, 50, 2625-2627.	13.8	114
21	Fourier-Transform Resonance Raman Spectroscopy of Intermediates of the Phytochrome Photocycle. Biochemistry, 1995, 34, 10497-10507.	2.5	109
22	Trinuclear Nickel Complexes with Triplesalen Ligands:Â Simultaneous Occurrence of Mixed Valence and Valence Tautomerism in the Oxidized Species. Inorganic Chemistry, 2005, 44, 5467-5482.	4.0	107
23	Novel Time-Resolved Surface-Enhanced (Resonance) Raman Spectroscopic Technique for Studying the Dynamics of Interfacial Processes: Application to the Electron Transfer Reaction of Cytochrome c at a Silver Electrode. Applied Spectroscopy, 1999, 53, 283-291.	2.2	106
24	Highly Conserved Residues Asp-197 and His-250 in Agp1 Phytochrome Control the Proton Affinity of the Chromophore and Pfr Formation. Journal of Biological Chemistry, 2007, 282, 2116-2123.	3.4	106
25	A Photochromic Histidine Kinase Rhodopsin (HKR1) That Is Bimodally Switched by Ultraviolet and Blue Light. Journal of Biological Chemistry, 2012, 287, 40083-40090.	3.4	106
26	Peripheral and Integral Binding of Cytochromecto Phospholipids Vesicles. Journal of Physical Chemistry B, 2004, 108, 3871-3878.	2.6	102
27	On the Electron Transfer Mechanism Between Cytochromecand Metal Electrodes. Evidence for Dynamic Control at Short Distancesâ€. Journal of Physical Chemistry B, 2006, 110, 19906-19913.	2.6	102
28	Spectroscopic Insights into the Oxygen-tolerant Membrane-associated [NiFe] Hydrogenase of Ralstonia eutropha H16. Journal of Biological Chemistry, 2009, 284, 16264-16276.	3.4	102
29	Why Does the Active Form of Galactose Oxidase Possess a Diamagnetic Ground State?. Angewandte Chemie - International Edition, 1998, 37, 616-619.	13.8	100
30	Cytochrome c-lipid interactions studied by resonance Raman and phosphorus-31 NMR spectroscopy. Correlation between the conformational changes of the protein and the lipid bilayer. Biochemistry, 1991, 30, 9084-9089.	2.5	99
31	The structural and functional role of lysine residues in the binding domain of cytochrome c in the electron transfer to cytochrome c oxidase. FEBS Journal, 1999, 261, 379-391.	0.2	98
32	Resonance Raman Spectroscopic Study of Metallochlorin Aggregates. Implications for the Supramolecular Structure in Chlorosomal BChl c Antennae of Green Bacteria. The Journal of Physical Chemistry, 1994, 98, 2192-2197.	2.9	97
33	Direct Observation of the Gating Step in Protein Electron Transfer: Electric-Field-Controlled Protein Dynamics. Journal of the American Chemical Society, 2008, 130, 9844-9848.	13.7	97
34	FellI-Hydroperoxo and Peroxo Complexes with Aminopyridyl Ligands and the Resonance Raman Spectroscopic Identification of the Feâ^'O and Oâ^'O Stretching Modes. European Journal of Inorganic Chemistry, 2000, 2000, 1627-1633.	2.0	93
35	Diastereoselective Control of BacteriochlorophylleAggregation. 31-S-BChleIs Essential for the Formation of Chlorosome-Like Aggregates. Journal of Physical Chemistry B, 2000, 104, 10379-10386.	2.6	93
36	Phenoxyl radical complexes of chromium(III), manganese(III), cobalt(III), and nickel(II). Inorganica Chimica Acta, 2000, 297, 265-277.	2.4	91

#	Article	IF	CITATIONS
37	Resonance Raman spectra of β-carotene in solution and in photosystems revisited: an experimental and theoretical study. Physical Chemistry Chemical Physics, 2009, 11, 11471.	2.8	90
38	The Chromophore Structural Changes during the Photocycle of Phytochrome:  A Combined Resonance Raman and Quantum Chemical Approach. Accounts of Chemical Research, 2007, 40, 258-266.	15.6	86
39	Cytochrome c at charged interfaces. 2. Complexes with negatively charged macromolecular systems studied by resonance Raman spectroscopy. Biochemistry, 1989, 28, 6722-6728.	2.5	85
40	Redox and Conformational Equilibria and Dynamics of Cytochrome c at High Electric Fields. ChemPhysChem, 2003, 4, 714-724.	2.1	85
41	Reversible [4Fe-3S] cluster morphing in an O2-tolerant [NiFe] hydrogenase. Nature Chemical Biology, 2014, 10, 378-385.	8.0	85
42	Analysis of vibrational spectra of multicomponent systems. Application to pH-dependent resonance Raman spectra of ferricytochrome c. Spectrochimica Acta - Part A: Molecular and Biomolecular Spectroscopy, 1996, 52, 573-584.	3.9	82
43	Determination of the Chromophore Structures in the Photoinduced Reaction Cycle of Phytochrome. Journal of the American Chemical Society, 2004, 126, 16734-16735.	13.7	82
44	A Selfâ€Improved Waterâ€Oxidation Catalyst: Is One Site Really Enough?. Angewandte Chemie - International Edition, 2014, 53, 205-209.	13.8	82
45	Raman Spectroscopic and Light-Induced Kinetic Characterization of a Recombinant Phytochrome of the Cyanobacterium Synechocystis. Biochemistry, 1997, 36, 13389-13395.	2.5	81
46	Anilino Radical Complexes of Cobalt(III) and Manganese(IV) and Comparison with Their Phenoxyl Analogues. Journal of the American Chemical Society, 2000, 122, 9663-9673.	13.7	81
47	Electrostatic-Field Dependent Activation Energies Modulate Electron Transfer of Cytochrome c. Journal of Physical Chemistry B, 2002, 106, 12814-12819.	2.6	81
48	Enhancement factor of surface-enhanced Raman scattering on silver and gold surfaces upon near-infrared excitation. Indication of an unusual strong contribution of the chemical effect. Journal of Raman Spectroscopy, 1993, 24, 791-796.	2.5	80
49	Conformational changes in cytochrome c and cytochrome oxidase upon complex formation: a resonance Raman study. Biochemistry, 1990, 29, 1661-1668.	2.5	77
50	Resonance Raman Spectroscopic Study of Phenoxyl Radical Complexes. Journal of the American Chemical Society, 1998, 120, 2352-2364.	13.7	77
51	Novel Auâ^'Ag Hybrid Device for Electrochemical SE(R)R Spectroscopy in a Wide Potential and Spectral Range. Nano Letters, 2009, 9, 298-303.	9.1	76
52	Cyanochromes Are Blue/Green Light Photoreversible Photoreceptors Defined by a Stable Double Cysteine Linkage to a Phycoviolobilin-type Chromophore. Journal of Biological Chemistry, 2009, 284, 29757-29772.	3.4	75
53	De novoDesign and Characterization of Copper Centers in Synthetic Four-Helix-Bundle Proteins. Journal of the American Chemical Society, 2001, 123, 2186-2195.	13.7	74
54	A protonation-coupled feedback mechanism controls the signalling process in bathy phytochromes. Nature Chemistry, 2015, 7, 423-430.	13.6	74

#	Article	IF	CITATIONS
55	Structure of the Full-Length Bacteriophytochrome from the Plant Pathogen Xanthomonas campestris Provides Clues to its Long-Range Signaling Mechanism. Journal of Molecular Biology, 2016, 428, 3702-3720.	4.2	73
56	The Fungal Phytochrome FphA from Aspergillus nidulans. Journal of Biological Chemistry, 2008, 283, 34605-34614.	3.4	71
57	A periplasmic aldehyde oxidoreductase represents the first molybdopterin cytosine dinucleotide cofactor containing molybdoâ€flavoenzyme from <i>Escherichia coli</i> . FEBS Journal, 2009, 276, 2762-2774.	4.7	71
58	Magnetic Silver Hybrid Nanoparticles for Surface-Enhanced Resonance Raman Spectroscopic Detection and Decontamination of Small Toxic Molecules. ACS Nano, 2013, 7, 3212-3220.	14.6	71
59	Quantum Mechanics/Molecular Mechanics Calculation of the Raman Spectra of the Phycocyanobilin Chromophore in α-C-Phycocyanin. Biophysical Journal, 2007, 93, 1885-1894.	0.5	70
60	NAD(H)â€coupled hydrogen cycling – structure–function relationships of bidirectional [NiFe] hydrogenases. FEBS Letters, 2012, 586, 545-556.	2.8	68
61	Photoconversion Mechanism of the Second GAF Domain of Cyanobacteriochrome AnPixJ and the Cofactor Structure of Its Green-Absorbing State. Biochemistry, 2013, 52, 4871-4880.	2.5	68
62	Quantitative conformational analysis of cytochromec bound to phospholipid vesicles studied by resonance Raman spectroscopy. European Biophysics Journal, 1990, 18, 193-201.	2.2	67
63	Proximal mutations at the typeÂ1 copper site of CotA laccase: spectroscopic, redox, kinetic and structural characterization of I494A and L386A mutants. Biochemical Journal, 2008, 412, 339-346.	3.7	66
64	Molecular Basis for the Electric Field Modulation of Cytochrome <i>c</i> Structure and Function. Journal of the American Chemical Society, 2009, 131, 16248-16256.	13.7	66
65	Chromophore Structure of Cyanobacterial Phytochrome Cph1 in the Pr State: Reconciling Structural and Spectroscopic Data by QM/MM Calculations. Biophysical Journal, 2009, 96, 4153-4163.	0.5	66
66	Assembly of photoactive orange carotenoid protein from its domains unravels a carotenoid shuttle mechanism. Photosynthesis Research, 2017, 133, 327-341.	2.9	66
67	Probing the Active Site of an O ₂ â€Tolerant NAD ⁺ â€Reducing [NiFe]â€Hydrogenase from <i>Ralstonia eutropha</i> H16 by Inâ€Situ EPR and FTIR Spectroscopy. Angewandte Chemie - International Edition, 2010, 49, 8026-8029.	13.8	65
68	Discrimination of Green Arabica and Robusta Coffee Beans by Raman Spectroscopy. Journal of Agricultural and Food Chemistry, 2010, 58, 11187-11192.	5.2	65
69	Metal-versusLigand-Centered Oxidations in Phenolatoâ^'Vanadium and â^'Cobalt Complexes:Â Characterization of Phenoxylâ^'Cobalt(III) Species. Inorganic Chemistry, 1997, 36, 3702-3710.	4.0	64
70	Chromophore Heterogeneity and Photoconversion in Phytochrome Crystals and Solution Studied by Resonance Raman Spectroscopy. Angewandte Chemie - International Edition, 2008, 47, 4753-4755.	13.8	64
71	Molecular Basis of Coupled Protein and Electron Transfer Dynamics of Cytochrome c in Biomimetic Complexes. Journal of the American Chemical Society, 2010, 132, 5769-5778.	13.7	64
72	Surfaceâ \in enhanced vibrational spectroscopy for probing transient interactions of proteins with biomimetic interfaces: electric field effects on structure, dynamics and function of cytochromeâ $\in f < i > c < /i >$. FEBS Journal, 2011, 278, 1382-1390.	4.7	64

#	Article	IF	CITATIONS
73	The Molecular and Electronic Structure of Symmetrically and Asymmetrically Coordinated, Non-Heme Iron Complexes Containing [FelIII(μ-N)FeIV]4+ (S=3/2) and [FeIV(μ-N)FeIV]5+ (S=0) Cores. Chemistry - A European Journal, 1999, 5, 793-810.	3.3	63
74	Electric-Field-Induced Redox Potential Shifts of Tetraheme Cytochromes c3 Immobilized on Self-Assembled Monolayers: Surface-Enhanced Resonance Raman Spectroscopy and Simulation Studies. Biophysical Journal, 2005, 88, 4188-4199.	0.5	63
75	Potentialâ€Dependent Surfaceâ€Enhanced Resonance Raman Spectroscopy at Nanostructured TiO ₂ : A Case Study on Cytochrome b ₅ . Small, 2013, 9, 4175-4181.	10.0	63
76	Surface-Enhanced Resonance Raman Spectroscopic and Electrochemical Study of Cytochrome c Bound on Electrodes through Coordination with Pyridinyl-Terminated Self-Assembled Monolayers. Journal of Physical Chemistry B, 2004, 108, 2261-2269.	2.6	62
77	Conformational transitions and redox potential shifts of cytochrome P450 induced by immobilization. Journal of Biological Inorganic Chemistry, 2006, 11, 119-127.	2.6	62
78	Redox-linked protein dynamics of cytochrome c probed by time-resolved surface enhanced infrared absorption spectroscopy. Physical Chemistry Chemical Physics, 2008, 10, 5276.	2.8	62
79	Structural snapshot of a bacterial phytochrome in its functional intermediate state. Nature Communications, 2018, 9, 4912.	12.8	62
80	Spectroelectrochemical Study of the [NiFe] Hydrogenase from Desulfovibrio vulgaris Miyazaki F in Solution and Immobilized on Biocompatible Gold Surfaces. Journal of Physical Chemistry B, 2009, 113, 15344-15351.	2.6	61
81	The Molecular and Electronic Structure of Octahedral Tris(phenolato)iron(III) Complexes and Their Phenoxyl Radical Analogues: A Mössbauer and Resonance Raman Spectroscopic Study. Chemistry - A European Journal, 1999, 5, 2554-2565.	3.3	60
82	Conformational and Redox Equilibria and Dynamics of CytochromecImmobilized on Electrodes via Hydrophobic Interactions. Journal of Physical Chemistry B, 2002, 106, 4823-4830.	2.6	60
83	Redox properties and catalytic activity of surface-bound human sulfite oxidase studied by a combined surface enhanced resonance Raman spectroscopic and electrochemical approach. Physical Chemistry Chemical Physics, 2010, 12, 7894.	2.8	60
84	Combined Electrochemistry and Surfaceâ€Enhanced Infrared Absorption Spectroscopy of Gramicidin A Incorporated into Tethered Bilayer Lipid Membranes. Angewandte Chemie - International Edition, 2012, 51, 8114-8117.	13.8	60
85	Resonance Raman Spectroscopy on [NiFe] Hydrogenase Provides Structural Insights into Catalytic Intermediates and Reactions. Journal of the American Chemical Society, 2014, 136, 9870-9873.	13.7	60
86	Long distance electron transfer in cytochrome c oxidase immobilised on electrodes. A surface enhanced resonance Raman spectroscopic study. Physical Chemistry Chemical Physics, 2006, 8, 759-766.	2.8	59
87	Vibrational Stark Effect of the Electric-Field Reporter 4-Mercaptobenzonitrile as a Tool for Investigating Electrostatics at Electrode/SAM/Solution Interfaces. International Journal of Molecular Sciences, 2012, 13, 7466-7482.	4.1	59
88	Structure of the Biliverdin Cofactor in the Pfr State of Bathy and Prototypical Phytochromes. Journal of Biological Chemistry, 2013, 288, 16800-16814.	3.4	58
89	Active site structure and redox processes of cytochrome c oxidase immobilised in a novel biomimetic lipid membrane on an electrode. Chemical Communications, 2004, , 2376.	4.1	57
90	Magnetic Titanium Dioxide Nanocomposites for Surfaceâ€Enhanced Resonance Raman Spectroscopic Determination and Degradation of Toxic Anilines and Phenols. Angewandte Chemie - International Edition, 2014, 53, 2481-2484.	13.8	57

#	Article	IF	CITATIONS
91	Protonation-Dependent Structural Heterogeneity in the Chromophore Binding Site of Cyanobacterial Phytochrome Cph1. Journal of Physical Chemistry B, 2017, 121, 47-57.	2.6	56
92	MerMAIDs: a family of metagenomically discovered marine anion-conducting and intensely desensitizing channelrhodopsins. Nature Communications, 2019, 10, 3315.	12.8	56
93	Chromophoreâ~Anion Interactions in Halorhodopsin fromNatronobacterium pharaonisProbed by Time-Resolved Resonance Raman Spectroscopyâ€. Biochemistry, 1997, 36, 11012-11020.	2.5	55
94	Electron transfer dynamics of cytochrome c bound to self-assembled monolayers on silver electrodes. Bioelectrochemistry, 2002, 55, 139-143.	4.6	55
95	Flexibility of human cytochrome P450 enzymes: Molecular dynamics and spectroscopy reveal important function-related variations. Biochimica Et Biophysica Acta - Proteins and Proteomics, 2011, 1814, 58-68.	2.3	55
96	Supramolecular Templates for Nanoflake–Metal Surfaces. Chemistry - A European Journal, 2009, 15, 2763-2767.	3.3	54
97	Light–Dark Adaptation of Channelrhodopsin Involves Photoconversion between the all- <i>trans</i> and 13- <i>cis</i> Retinal Isomers. Biochemistry, 2015, 54, 5389-5400.	2.5	54
98	Probing Structure and Reaction Dynamics of Proteins Using Time-Resolved Resonance Raman Spectroscopy. Chemical Reviews, 2020, 120, 3577-3630.	47.7	54
99	Time-Resolved Surface-Enhanced Resonance Raman Spectroscopy for Studying Electron-Transfer Dynamics of Heme Proteins. Journal of the American Chemical Society, 1998, 120, 7381-7382.	13.7	53
100	Carbamoylphosphate serves as the source of CNâ^', but not of the intrinsic CO in the active site of the regulatory [NiFe]-hydrogenase fromRalstonia eutropha. FEBS Letters, 2007, 581, 3322-3326.	2.8	53
101	Resonance Raman Spectroscopy as a Tool to Monitor the Active Site of Hydrogenases. Angewandte Chemie - International Edition, 2013, 52, 5162-5165.	13.8	53
102	Active-Site Structure and Dynamics of Cytochrome c Immobilized on Self-Assembled Monolayers-A Time-Resolved Surface Enhanced Resonance Raman Spectroscopic Study. Angewandte Chemie - International Edition, 2001, 40, 728-731.	13.8	52
103	Vibrational spectroscopy reveals the initial steps of biological hydrogen evolution. Chemical Science, 2016, 7, 6746-6752.	7.4	52
104	(Photo)ionization of tris(phenolato)iron(III) complexes: generation of phenoxyl radical as ligand. Journal of the American Chemical Society, 1993, 115, 11222-11230.	13.7	51
105	Characterization of Two Thermostable Cyanobacterial Phytochromes Reveals Global Movements in the Chromophore-binding Domain during Photoconversion. Journal of Biological Chemistry, 2008, 283, 21251-21266.	3.4	51
106	μ-Nitridodiiron Complexes with Asymmetric[FelVN-FellI]4+ and Symmetric[FelVNFelV]5+ Structural Elements. Angewandte Chemie International Edition in English, 1995, 34, 669-672.	4.4	49
107	Conformational equilibria and dynamics of cytochrome c induced by binding of sodium dodecyl sulfate monomers and micelles. European Biophysics Journal, 2003, 32, 599-613.	2.2	49
108	Mesoporous Indium Tin Oxide as a Novel Platform for Bioelectronics. ChemCatChem, 2010, 2, 839-845.	3.7	49

#	Article	IF	CITATIONS
109	The role of Glu498 in the dioxygen reactivity of CotA-laccase from Bacillus subtilis. Dalton Transactions, 2010, 39, 2875.	3.3	49
110	SEIRA Spectroscopy of the Electrochemical Activation of an Immobilized [NiFe] Hydrogenase under Turnover and Nonâ€Turnover Conditions. Angewandte Chemie - International Edition, 2011, 50, 2632-2634.	13.8	48
111	Dinuclear Copper Complexes Based on Parallel β-Diiminato Binding Sites and their Reactions with O ₂ : Evidence for a Cuâ^Oâ^Cu Entity. Inorganic Chemistry, 2011, 50, 2133-2142.	4.0	47
112	Comparative resonance Raman study of cytochrome c oxidase from beef heart and Paracoccus denitrificans. Biochemistry, 1993, 32, 10866-10877.	2.5	46
113	Monitoring Catalysis of the Membraneâ€Bound Hydrogenase from <i>Ralstonia eutropha</i> H16 by Surfaceâ€Enhanced IR Absorption Spectroscopy. Angewandte Chemie - International Edition, 2009, 48, 611-613.	13.8	46
114	Resonance Raman study of the interactions between cytochrome c variants and cytochrome c oxidase. Biochemistry, 1993, 32, 10912-10922.	2.5	45
115	Gated Electron Transfer of Yeast Iso-1 Cytochrome c on Self-Assembled Monolayer-Coated Electrodes. Journal of Physical Chemistry B, 2008, 112, 15202-15211.	2.6	45
116	Structural changes of myoglobin in pressure-treated pork meat probed by resonance Raman spectroscopy. Food Chemistry, 2009, 115, 1194-1198.	8.2	45
117	Electric-Field Control of the pH-Dependent Redox Process of Cytochrome <i>c</i> Immobilized on a Gold Electrode. Journal of Physical Chemistry C, 2012, 116, 13038-13044.	3.1	45
118	Unusual Spectral Properties of Bacteriophytochrome Agp2 Result from a Deprotonation of the Chromophore in the Red-absorbing Form Pr. Journal of Biological Chemistry, 2013, 288, 31738-31751.	3.4	45
119	Redox Processes of CytochromecImmobilized on Solid Supported Polyelectrolyte Multilayers. Journal of Physical Chemistry B, 2006, 110, 522-529.	2.6	44
120	Concerted Action of Two Novel Auxiliary Proteins in Assembly of the Active Site in a Membrane-bound [NiFe] Hydrogenase. Journal of Biological Chemistry, 2009, 284, 2159-2168.	3.4	44
121	A Red/Green Cyanobacteriochrome Sustains Its Color Despite a Change in the Bilin Chromophore's Protonation State. Biochemistry, 2015, 54, 5839-5848.	2.5	44
122	Fourier transform resonance Raman spectroscopy of phytochrome. Biochemistry, 1992, 31, 7957-7962.	2.5	43
123	Resonance Raman spectroscopy of sensory rhodopsin II from Natronobacterium pharaonis. FEBS Letters, 2000, 472, 263-266.	2.8	43
124	DsrJ, an Essential Part of the DsrMKJOP Transmembrane Complex in the Purple Sulfur Bacterium <i>Allochromatium vinosum</i> , Is an Unusual Triheme Cytochrome <i>c</i> . Biochemistry, 2010, 49, 8290-8299.	2.5	43
125	Vibrational analysis of biliverdin dimethyl ester. The Journal of Physical Chemistry, 1993, 97, 11887-11900.	2.9	42
126	Reduction of Unusual Iron-Sulfur Clusters in the H2-sensing Regulatory Ni-Fe Hydrogenase from Ralstonia eutropha H16. Journal of Biological Chemistry, 2005, 280, 19488-19495.	3.4	42

#	Article	IF	CITATIONS
127	Heme Coordination States of Unfolded Ferrous Cytochrome c. Biophysical Journal, 2006, 91, 3022-3031.	0.5	42
128	Temperature Dependence of the Catalytic Two- versus Four-Electron Reduction of Dioxygen by a Hexanuclear Cobalt Complex. Journal of the American Chemical Society, 2017, 139, 15033-15042.	13.7	42
129	Binding of Azole Antibiotics to Staphylococcus aureus Flavohemoglobin Increases Intracellular Oxidative Stress. Journal of Bacteriology, 2010, 192, 1527-1533.	2.2	41
130	Spectroscopic and Photochemical Characterization of the Redâ€Light Sensitive Photosensory Module of Cph2 from <i>Synechocystis</i> PCC 6803. Photochemistry and Photobiology, 2011, 87, 160-173.	2.5	41
131	A Highâ€Valent Heterobimetallic [Cu ^{III} (μâ€O) ₂ Ni ^{III}] ²⁺ Core with Nucleophilic Oxo Groups. Angewandte Chemie - International Edition, 2013, 52, 5622-5626.	13.8	41
132	High Performance Reduction of H ₂ O ₂ with an Electron Transport Decaheme Cytochrome on a Porous ITO Electrode. Journal of the American Chemical Society, 2017, 139, 3324-3327.	13.7	41
133	Determination of the Local Electric Field at Au/SAM Interfaces Using the Vibrational Stark Effect. Journal of Physical Chemistry C, 2017, 121, 22274-22285.	3.1	41
134	Raman excitation profiles of <i>l²</i> â€carotene – novel insights into the nature of the <i>l1⁄2</i> ₁ â€band. Physica Status Solidi (B): Basic Research, 2008, 245, 2225-2228.	1.5	40
135	Site Directed Mutagenesis of Amino Acid Residues at the Active Site of Mouse Aldehyde Oxidase AOX1. PLoS ONE, 2009, 4, e5348.	2.5	40
136	Role of Met80 and Tyr67 in the Low-pH Conformational Equilibria of Cytochrome <i>c</i> . Biochemistry, 2012, 51, 5967-5978.	2.5	40
137	Calculation of Vibrational Spectra of Linear Tetrapyrroles. 1. Global Sets of Scaling Factors for Force Fields Derived by ab Initio and Density Functional Theory Methods. Journal of Physical Chemistry A, 1999, 103, 289-303.	2.5	39
138	Induced SERâ€Activity in Nanostructured Ag–Silica–Au Supports via Longâ€Range Plasmon Coupling. Advanced Functional Materials, 2010, 20, 1954-1961.	14.9	39
139	Role of the HoxZ Subunit in the Electron Transfer Pathway of the Membrane-Bound [NiFe]-Hydrogenase from <i>Ralstonia eutropha</i> Immobilized on Electrodes. Journal of Physical Chemistry B, 2011, 115, 10368-10374.	2.6	39
140	Interpretation of the resonance Raman spectra of linear tetrapyrroles based on DFT calculations. Chemical Physics Letters, 1999, 311, 479-484.	2.6	38
141	Midpoint Potentials of Hemesaanda3in the Quinol Oxidase fromAcidianus ambivalensare Inverted. Journal of the American Chemical Society, 2005, 127, 13561-13566.	13.7	38
142	The Mechanism of Assembly and Cofactor Insertion into Rhodobacter capsulatus Xanthine Dehydrogenase. Journal of Biological Chemistry, 2008, 283, 16602-16611.	3.4	38
143	Electric-field effects on the interfacial electron transfer and protein dynamics of cytochrome c. Journal of Electroanalytical Chemistry, 2011, 660, 367-376.	3.8	38
144	Structure of the Chromophore Binding Pocket in the Pr State of Plant Phytochrome phyA. Journal of Physical Chemistry B, 2011, 115, 1220-1231.	2.6	38

#	Article	IF	CITATIONS
145	Voltage-dependent structural changes of the membrane-bound anion channel hVDAC1 probed by SEIRA and electrochemical impedance spectroscopy. Physical Chemistry Chemical Physics, 2014, 16, 9546-9555.	2.8	38
146	Polyanion binding to cytochrome c probed by resonance Raman spectroscopy. BBA - Proteins and Proteomics, 1990, 1040, 175-186.	2.1	37
147	Characterization of an Alkaline Transition Intermediate Stabilized in the Phe82Trp Variant of Yeastiso-1-Cytochromecâ€. Biochemistry, 2000, 39, 9047-9054.	2.5	37
148	Spectroscopic Identification of Different Types of Copper Centers Generated in Synthetic Four-Helix Bundle Proteins. Journal of the American Chemical Society, 2004, 126, 14389-14399.	13.7	37
149	Surface enhanced resonance Raman study on fluorescein dyes. Journal of Raman Spectroscopy, 1986, 17, 55-58.	2.5	36
150	Dynamics of the Heterogeneous Electron-Transfer Reaction of Cytochrome c552 from Thermus thermophilus. A Time-Resolved Surface-Enhanced Resonance Raman Spectroscopic Study. Journal of Physical Chemistry B, 1999, 103, 10053-10064.	2.6	36
151	Thermal Fluctuations Determine the Electronâ€Transfer Rates of Cytochrome c in Electrostatic and Covalent Complexes. ChemPhysChem, 2010, 11, 1225-1235.	2.1	36
152	Perturbation of the Redox Site Structure of Cytochrome c Variants upon Tyrosine Nitration. Journal of Physical Chemistry B, 2012, 116, 5694-5702.	2.6	36
153	Polarization- and Wavelength-Dependent Surface-Enhanced Raman Spectroscopy Using Optically Anisotropic Rippled Substrates for Sensing. ACS Sensors, 2016, 1, 318-323.	7.8	36
154	Fourier transform near-infrared resonance Raman spectroscopic study of the α-subunit of phycoerythrocyanin and phycocyanin from the cyanobacteriumMastigocladus laminosus. Journal of Raman Spectroscopy, 1998, 29, 939-944.	2.5	35
155	SERR-Spectroelectrochemical Study of a <i>cbb</i> ₃ Oxygen Reductase in a Biomimetic Construct. Journal of Physical Chemistry B, 2008, 112, 16952-16959.	2.6	35
156	Interfacial redox processes of cytochrome b562. Physical Chemistry Chemical Physics, 2009, 11, 7430.	2.8	35
157	Reversible Active Site Sulfoxygenation Can Explain the Oxygen Tolerance of a NAD ⁺ -Reducing [NiFe] Hydrogenase and Its Unusual Infrared Spectroscopic Properties. Journal of the American Chemical Society, 2015, 137, 2555-2564.	13.7	35
158	Monitoring the Orientational Changes of Alamethicin during Incorporation into Bilayer Lipid Membranes. Langmuir, 2018, 34, 2373-2385.	3.5	35
159	The Chromophore Structures of the Pr States in Plant and Bacterial Phytochromes. Biophysical Journal, 2007, 93, 2410-2417.	0.5	34
160	Gated electron transfer of cytochrome c6 at biomimetic interfaces: a time-resolved SERR study. Physical Chemistry Chemical Physics, 2009, 11, 7390.	2.8	34
161	Analyzing the catalytic processes of immobilized redox enzymes by vibrational spectroscopies. IUBMB Life, 2012, 64, 455-464.	3.4	33
162	Monitoring the Transmembrane Proton Gradient Generated by Cytochrome <i>bo</i> ₃ in Tethered Bilayer Lipid Membranes Using SEIRA Spectroscopy. Journal of Physical Chemistry B, 2016, 120, 2249-2256.	2.6	33

#	Article	IF	CITATIONS
163	Robust electrografted interfaces on metal oxides for electrocatalysis – an <i>in situ</i> spectroelectrochemical study. Journal of Materials Chemistry A, 2018, 6, 15200-15212.	10.3	33
164	Computer simulation and SERR detection of cytochrome c dynamics at SAM-coated electrodes. Electrochimica Acta, 2009, 54, 4963-4970.	5.2	32
165	Unraveling the Interfacial Electron Transfer Dynamics of Electroactive Microbial Biofilms Using Surfaceâ€Enhanced Raman Spectroscopy. ChemSusChem, 2013, 6, 487-492.	6.8	32
166	Electrocatalytic Oxygen Evolution Reaction on Iridium Oxide Model Film Catalysts: Influence of Oxide Type and Catalyst Substrate Interactions. ECS Transactions, 2013, 58, 39-51.	0.5	32
167	Structural Parameters Controlling the Fluorescence Properties of Phytochromes. Biochemistry, 2014, 53, 20-29.	2.5	32
168	Mimicking Tyrosine Phosphorylation in Human Cytochromeâ€ <i>c</i> by the Evolved tRNA Synthetase Technique. Chemistry - A European Journal, 2015, 21, 15004-15012.	3.3	32
169	Iron–sulfur repair YtfE protein from Escherichia coli: structural characterization of the di-iron center. Journal of Biological Inorganic Chemistry, 2008, 13, 765-770.	2.6	31
170	Lightâ€Induced Activation of Bacterial Phytochrome Agp1 Monitored by Static and Timeâ€Resolved FTIR Spectroscopy. ChemPhysChem, 2010, 11, 1207-1214.	2.1	31
171	Escherichia coli RIC Is Able to Donate Iron to Iron-Sulfur Clusters. PLoS ONE, 2014, 9, e95222.	2.5	31
172	Effect of chromophore exchange on the resonance Raman spectra of recombinant phytochromes. FEBS Letters, 1997, 414, 23-26.	2.8	30
173	FTIR Study of the Photoinduced Processes of Plant Phytochrome Phya using Isotope-Labeled Bilins and Density Functional Theory Calculations. Biophysical Journal, 2008, 95, 1256-1267.	0.5	30
174	The impact of urea-induced unfolding on the redox process of immobilised cytochrome c. Journal of Biological Inorganic Chemistry, 2010, 15, 1233-1242.	2.6	30
175	Elucidating photoinduced structural changes in phytochromes by the combined application of resonance Raman spectroscopy and theoretical methods. Journal of Molecular Structure, 2011, 993, 15-25.	3.6	30
176	Resonance Raman Spectroscopic Analysis of the [NiFe] Active Site and the Proximal [4Fe-3S] Cluster of an O ₂ -Tolerant Membrane-Bound Hydrogenase in the Crystalline State. Journal of Physical Chemistry B, 2015, 119, 13785-13796.	2.6	30
177	Controlled Microwave-Hydrolyzed Starch as a Stabilizer for Green Formulation of Aqueous Gold Nanoparticle Ink for Flexible Printed Electronics. ACS Applied Nano Materials, 2018, 1, 1247-1256.	5.0	30
178	Long-Range Modulations of Electric Fields in Proteins. Journal of Physical Chemistry B, 2018, 122, 8330-8342.	2.6	30
179	Ultraviolet resonance Raman spectroscopy of formamide: evidence for npi.* interferences and intermolecular vibronic coupling. The Journal of Physical Chemistry, 1990, 94, 2274-2279.	2.9	29
180	The heterogeneous electron transfer of cytochrome c adsorbed on Ag electrodes coated with ï‰-carboxyl alkanethiols. A surface enhanced resonance Raman spectroscopic study. Journal of Molecular Structure, 2001, 565-566, 97-100.	3.6	29

#	Article	IF	CITATIONS
181	Characterization and Crystallization of Mouse Aldehyde Oxidase 3: From Mouse Liver to <i>Escherichia coli</i> Heterologous Protein Expression. Drug Metabolism and Disposition, 2011, 39, 1939-1945.	3.3	29
182	Orientation-Controlled Electrocatalytic Efficiency of an Adsorbed Oxygen-Tolerant Hydrogenase. PLoS ONE, 2015, 10, e0143101.	2.5	29
183	Improved Method for the Incorporation of Heme Cofactors into Recombinant Proteins Using <i>Escherichia coli</i> Nissle 1917. Biochemistry, 2018, 57, 2747-2755.	2.5	29
184	Chemical Exchange and Raman Line Broadening. The Rate of Protolysis of Nitric Acid. Zeitschrift Fur Elektrotechnik Und Elektrochemie, 1983, 87, 516-522.	0.9	28
185	Dynamics and mechanism of the electron transfer process of cytochrome c probed by resonance Raman and surface enhanced resonance Raman spectroscopy. Journal of Molecular Structure, 2001, 563-564, 51-59.	3.6	28
186	Electron Transfer in SAM/Cytochrome/Polyelectrolyte Hybrid Systems on Electrodes:  A Time-Resolved Surface-Enhanced Resonance Raman Study. Langmuir, 2007, 23, 11289-11294.	3.5	28
187	Novel cylindrical rotating electrode for anaerobic surface-enhanced Raman spectroscopy. Journal of Raman Spectroscopy, 1988, 19, 65-69.	2.5	27
188	Resonance Raman Spectroscopic Evidence for the Identity of the Bacteriochlorophyll c Organization in Protein-Free and Protein-Containing Chlorosomes from Chloroflexus auvantiacus. Zeitschrift Fur Naturforschung - Section C Journal of Biosciences, 1991, 46, 228-232.	1.4	27
189	Calculation of the Vibrational Spectra of Linear Tetrapyrroles. 2. Resonance Raman Spectra of Hexamethylpyrromethene Monomersâ€. Journal of Physical Chemistry B, 2000, 104, 10885-10899.	2.6	27
190	Molecular effects of highâ€pressure processing on food studied by resonance Raman. Annals of the New York Academy of Sciences, 2010, 1189, 34-42.	3.8	27
191	Stoichiometric Formation of an Oxoiron(IV) Complex by a Soluble Methane Monooxygenase Type Activation of O ₂ at an Iron(II)-Cyclam Center. Journal of the American Chemical Society, 2020, 142, 5924-5928.	13.7	27
192	Resonance Raman spectroscopic study of the neutral flavin radical complex of DNA photolyase fromEscherichia coli. Journal of Raman Spectroscopy, 2001, 32, 551-556.	2.5	26
193	Electrochemical and Spectroscopic Investigations of Immobilized De Novo Designed Heme Proteins on Metal Electrodes. ChemPhysChem, 2005, 6, 961-970.	2.1	26
194	The structure of the Ni-Fe site in the isolated HoxC subunit of the hydrogen-sensing hydrogenase fromRalstonia eutropha. FEBS Letters, 2005, 579, 4287-4291.	2.8	26
195	Electrochemical Response of Cytochrome <i>c</i> Immobilized on Smooth and Roughened Silver and Gold Surfaces Chemically Modified with 11-Mercaptounodecanoic Acid. Journal of Physical Chemistry C, 2009, 113, 2861-2866.	3.1	26
196	Disentangling Electron Tunneling and Protein Dynamics of Cytochrome c through a Rationally Designed Surface Mutation. Journal of Physical Chemistry B, 2013, 117, 6061-6068.	2.6	26
197	NirN Protein from Pseudomonas aeruginosa is a Novel Electron-bifurcating Dehydrogenase Catalyzing the Last Step of Heme d1 Biosynthesis. Journal of Biological Chemistry, 2014, 289, 30753-30762.	3.4	26
198	Conformational heterogeneity of the Pfr chromophore in plant and cyanobacterial phytochromes. Frontiers in Molecular Biosciences, 2015, 2, 37.	3.5	26

#	Article	IF	CITATIONS
199	A New Domain of Reactivity for Highâ€Valent Dinuclear [M(μâ€O) ₂ Mâ€2] Complexes in Oxidation Reactions. Angewandte Chemie - International Edition, 2017, 56, 297-301.	13.8	26
200	The Photoconversion of Phytochrome Includes an Unproductive Shunt Reaction Pathway. ChemPhysChem, 2018, 19, 566-570.	2.1	26
201	Protein-protein interactions in microsomal cytochrome P-450 isozyme LM2 and their effect on substrate binding. FEBS Journal, 1989, 186, 383-388.	0.2	25
202	Cytochrome c and cytochrome c peroxidase complex as studied by resonance Raman spectroscopy. Biochemistry, 1992, 31, 2384-2392.	2.5	25
203	Carbon Nanotube Bags: Catalytic Formation, Physical Properties, Two-Dimensional Alignment and Geometric Structuring of Densely Filled Carbon Tubes. Chemistry - A European Journal, 2001, 7, 2888-2895.	3.3	25
204	A Spectral Window to the Cell. Angewandte Chemie - International Edition, 2010, 49, 4540-4541.	13.8	25
205	Surface-enhanced resonance Raman spectroscopy of copper chlorophyllin on silver and gold colloids. The Journal of Physical Chemistry, 1988, 92, 3355-3360.	2.9	24
206	Conformational Analysis of Mitochondrial and Microsomal Cytochrome P-450 by Resonance Raman Spectroscopy. Biochemistry, 1994, 33, 12920-12929.	2.5	24
207	The cytochrome ba complex from the thermoacidophilic crenarchaeote Acidianus ambivalens is an analog of bc1 complexes. Biochimica Et Biophysica Acta - Bioenergetics, 2009, 1787, 37-45.	1.0	24
208	Comparison of the membrane-bound [NiFe] hydrogenases from R. eutropha H16 and D. vulgaris Miyazaki F in the oxidized ready state by pulsed EPR. Physical Chemistry Chemical Physics, 2010, 12, 2139.	2.8	24
209	Structural changes in cytochrome c upon hydrogen-deuterium exchange. Biochemistry, 1993, 32, 14158-14164.	2.5	23
210	Structural Similarities and Differences of the Heme Pockets of Various P450 Isoforms as Revealed by Resonance Raman Spectroscopy. Archives of Biochemistry and Biophysics, 2000, 383, 70-78.	3.0	23
211	Multi-layer electron transfer across nanostructured Ag-SAM-Au-SAM junctions probed by surface enhanced Raman spectroscopy. Physical Chemistry Chemical Physics, 2010, 12, 9822.	2.8	23
212	Mapping local electric fields in proteins at biomimetic interfaces. Chemical Communications, 2012, 48, 70-72.	4.1	23
213	In Situ Spectroelectrochemical Studies into the Formation and Stability of Robust Diazonium-Derived Interfaces on Gold Electrodes for the Immobilization of an Oxygen-Tolerant Hydrogenase. ACS Applied Materials & Interfaces, 2018, 10, 23380-23391.	8.0	23
214	Raman spectroscopic study of the conformational changes of thyroxine induced by interactions with phospholipid. European Biophysics Journal, 2002, 31, 448-453.	2.2	22
215	Silver Nanocoral Structures on Electrodes:  A Suitable Platform for Protein-Based Bioelectronic Devices. Langmuir, 2008, 24, 1583-1586.	3.5	22
216	Effect of the Protonation Degree of a Self-Assembled Monolayer on the Immobilization Dynamics of a [NiFe] Hydrogenase. Langmuir, 2013, 29, 673-682.	3.5	22

#	Article	IF	CITATIONS
217	When the inhibitor tells more than the substrate: the cyanide-bound state of a carbon monoxide dehydrogenase. Chemical Science, 2016, 7, 3162-3171.	7.4	22
218	Structural insights into photoactivation and signalling in plant phytochromes. Nature Plants, 2020, 6, 581-588.	9.3	22
219	An Sâ€Oxygenated [NiFe] Complex Modelling Sulfenate Intermediates of an O ₂ â€Tolerant Hydrogenase. Angewandte Chemie - International Edition, 2017, 56, 2208-2211.	13.8	21
220	Common Structural Elements in the Chromophore Binding Pocket of the Pfr State of Bathy Phytochromes. Photochemistry and Photobiology, 2017, 93, 724-732.	2.5	21
221	Freeze-Quench Resonance Raman and Electron Paramagnetic Resonance Spectroscopy for Studying Enzyme Kinetics: Application to Azide Binding to Myoglobin. Applied Spectroscopy, 2000, 54, 1480-1484.	2.2	20
222	Calculation of Vibrational Spectra of Linear Tetrapyrroles. 3. Hydrogen-Bonded Hexamethylpyrromethene Dimers. Journal of Physical Chemistry A, 2005, 109, 2139-2150.	2.5	20
223	Image dipoles approach to the local field enhancement in nanostructured Ag–Au hybrid devices. Journal of Chemical Physics, 2010, 132, 024712.	3.0	20
224	Revealing the Absolute Configuration of the CO and CN ^{â^'} Ligands at the Active Site of a [NiFe] Hydrogenase. ChemPhysChem, 2012, 13, 3852-3856.	2.1	20
225	ATP-induced electron transfer by redox-selective partner recognition. Nature Communications, 2014, 5, 4626.	12.8	20
226	The large subunit of the regulatory [NiFe]-hydrogenase fromRalstonia eutropha– a minimal hydrogenase?. Chemical Science, 2020, 11, 5453-5465.	7.4	20
227	Redox processes in pressurised smoked salmon studied by resonance Raman spectroscopy. Food Chemistry, 2009, 112, 482-486.	8.2	19
228	The chromophore structure of the long-lived intermediate of the C128T channelrhodopsin-2 variant. FEBS Letters, 2011, 585, 3998-4001.	2.8	19
229	The role of local and remote amino acid substitutions for optimizing fluorescence in bacteriophytochromes: A case study on iRFP. Scientific Reports, 2016, 6, 28444.	3.3	19
230	Using Separable Nonnegative Matrix Factorization Techniques for the Analysis of Time-Resolved Raman Spectra. Applied Spectroscopy, 2016, 70, 1464-1475.	2.2	19
231	The anomaly of the \$u\$ ₁ â€resonance Raman band of bβâ€carotene in solution and in photosystem I and II. Physica Status Solidi (B): Basic Research, 2009, 246, 2790-2793.	1.5	18
232	Raman Spectra of the Phycoviolobilin Cofactor in Phycoerythrocyanin Calculated by QM/MM Methods. ChemPhysChem, 2010, 11, 1265-1274.	2.1	18
233	Theory of time-resolved Raman scattering and fluorescence emission from semiconductor quantum dots. Physical Review B, 2010, 81, .	3.2	18
234	Redox-dependent substrate-cofactor interactions in the Michaelis-complex of a flavin-dependent oxidoreductase. Nature Communications, 2017, 8, .	12.8	18

#	Article	IF	CITATIONS
235	The C-Terminal VPRTES Tail of LL-37 Influences the Mode of Attachment to a Lipid Bilayer and Antimicrobial Activity. Biochemistry, 2019, 58, 2447-2462.	2.5	18
236	Red, Orange, Green: Light- and Temperature-Dependent Color Tuning in a Cyanobacteriochrome. Biochemistry, 2020, 59, 509-519.	2.5	18
237	Immobilized dye-decolorizing peroxidase (DyP) and directed evolution variants for hydrogen peroxide biosensing. Biosensors and Bioelectronics, 2020, 153, 112055.	10.1	18
238	Resonance Raman study on the structure of the active sites of microsomal cytochrome P-450 isozymes LM2 and LM4. FEBS Journal, 1989, 186, 291-302.	0.2	17
239	Unusual heme structure in cytochrome aa3 from Sulfolobus acidocaldarius: A resonance Raman investigation. Biochemistry, 1993, 32, 10878-10884.	2.5	17
240	The active site structure ofba3 oxidase fromThermus thermophilus studied by resonance Raman spectroscopy. , 1999, 5, S53-S63.		17
241	Bias from H2Cleavage to Production and Coordination Changes at the Niâ^Fe Active Site in the NAD+-Reducing Hydrogenase fromRalstonia eutrophaâ€. Biochemistry, 2006, 45, 11658-11665.	2.5	17
242	Voltammetry and in situ scanning tunnelling microscopy of de novo designed heme protein monolayers on Au(111)-electrode surfaces. Bioelectrochemistry, 2006, 69, 193-200.	4.6	17
243	Time-resolved resonance Raman spectroscopy of sensory rhodopsin II in the micro- and millisecond time range using gated cw excitation. Journal of Raman Spectroscopy, 2006, 37, 436-441.	2.5	17
244	Surface enhanced vibrational spectroscopic evidence for an alternative DNA-independent redox activation of endonuclease III. Chemical Communications, 2015, 51, 3255-3257.	4.1	17
245	Nickel electrodes as a cheap and versatile platform for studying structure and function of immobilized redox proteins. Analytica Chimica Acta, 2016, 941, 35-40.	5.4	17
246	Hydroxy-bridged resting states of a [NiFe]-hydrogenase unraveled by cryogenic vibrational spectroscopy and DFT computations. Chemical Science, 2021, 12, 2189-2197.	7.4	17
247	Resonance Raman spectroscopic studies of cytochrome c at charged interfaces. Journal of Molecular Structure, 1991, 242, 379-395.	3.6	16
248	Raman spectroscopic analysis of isomers of biliverdin dimethyl ester. Journal of Pharmaceutical and Biomedical Analysis, 1997, 15, 1319-1324.	2.8	16
249	Calculation of Vibrational Spectra of Linear Tetrapyrroles. 4. Methine Bridge Câ^'H Out-of-Plane Modes. Journal of Physical Chemistry A, 2006, 110, 10564-10574.	2.5	16
250	A Spectroscopic Study of the Temperature Induced Modifications on Ferredoxin Folding and Ironâ^'Sulfur Moieties. Biochemistry, 2007, 46, 10733-10738.	2.5	16
251	Electrosynthesis of SER-Active Silver Nanopillar Electrode Arrays. Journal of Physical Chemistry C, 2010, 114, 7280-7284.	3.1	16
252	Insights into the structure of the active site of the O2-tolerant membrane bound [NiFe] hydrogenase of R. eutropha H16 by molecular modelling. Physical Chemistry Chemical Physics, 2011, 13, 16146.	2.8	16

#	Article	IF	CITATIONS
253	Orthogonal Translation Meets Electron Transfer: In Vivo Labeling of Cytochrome <i>c</i> for Probing Local Electric Fields. ChemBioChem, 2015, 16, 742-745.	2.6	16
254	Structural and Vibrational Characterization of the Chromophore Binding Site of Bacterial Phytochrome Agp1. Photochemistry and Photobiology, 2017, 93, 713-723.	2.5	16
255	Gradient metal nanoislands as a unified surface enhanced Raman scattering and surface enhanced infrared absorption platform for analytics. Analyst, The, 2019, 144, 5271-5276.	3.5	16
256	A Pseudotetrahedral Terminal Oxoiron(IV) Complex: Mechanistic Promiscuity in Câ^'H Bond Oxidation Reactions. Angewandte Chemie - International Edition, 2021, 60, 6752-6756.	13.8	16
257	Spectroscopic Characterization of a Reactive [Cu ₂ (μâ€OH) ₂] ²⁺ Intermediate in Cu/TEMPO Catalyzed Aerobic Alcohol Oxidation Reaction. Angewandte Chemie - International Edition, 2021, 60, 23018-23024.	13.8	16
258	Unusual structures and unknown roles of FeS clusters in metalloenzymes seen from a resonance Raman spectroscopic perspective. Coordination Chemistry Reviews, 2022, 452, 214287.	18.8	16
259	Surface enhanced resonance Raman study of phenobarbital-induced rabbit liver cytochrome P-450 LM2. FEBS Letters, 1988, 227, 76-80.	2.8	15
260	Active sites of two orthologous cytochromes P450 2E1: Differences revealed by spectroscopic methods. Biochemical and Biophysical Research Communications, 2005, 338, 477-482.	2.1	15
261	The Photoreactions of Recombinant Phytochrome CphA from the Cyanobacterium <i>Calothrix</i> PCC7601: A Lowâ€Temperature UV–Vis and FTIR Study. Photochemistry and Photobiology, 2009, 85, 239-249.	2.5	15
262	Substrate Binding to a Nitrite Reductase Induces a Spin Transition. Journal of Physical Chemistry B, 2010, 114, 5563-5566.	2.6	15
263	Desulforubrerythrin from Campylobacter jejuni, a novel multidomain protein. Journal of Biological Inorganic Chemistry, 2011, 16, 501-510.	2.6	15
264	Photochemical chromophore isomerization in histidine kinase rhodopsin HKR1. FEBS Letters, 2015, 589, 1067-1071.	2.8	15
265	Reversible light-dependent molecular switches on Ag/AgCl nanostructures. Nanoscale, 2017, 9, 8380-8387.	5.6	15
266	Chromophore binding to two cysteines increases quantum yield of near-infrared fluorescent proteins. Scientific Reports, 2019, 9, 1866.	3.3	15
267	Resonance Raman study of cytochrome aa 3 from Sulfolobus acidocaldarius. FEBS Letters, 1991, 283, 131-134.	2.8	14
268	Potential-dependent surface enhanced resonance Raman spectroscopy of cytochromec552 fromThermus thermophilus. Journal of Raman Spectroscopy, 1998, 29, 687-692.	2.5	14
269	Resonance Raman spectroscopic study of thecaa3 oxidase fromThermus thermophilus. , 1998, 4, 365-377.		14
270	Spectroscopic and structural properties of N -sulfinyl-benzenamine, O S N–C 6 H 5. Journal of Molecular Structure, 1999, 508, 5-17.	3.6	14

#	Article	IF	CITATIONS
271	Structural Changes of Cytochromec552 fromThermus thermophilus Adsorbed on Anionic and Hydrophobic Surfaces Probed by FTIR and 2D-FTIR Spectroscopy. ChemBioChem, 2001, 2, 180-189.	2.6	14
272	Comparative vibrational analysis of thyronine hormones using infrared and Raman spectroscopy and density functional theory calculations. Journal of Raman Spectroscopy, 2004, 35, 947-955.	2.5	14
273	Regioselective Deuteration and Resonance Raman Spectroscopic Characterization of Biliverdin and Phycocyanobilin. Chemistry - A European Journal, 1997, 3, 363-367.	3.3	14
274	Complex Formation with the Activator RACo Affects the Corrinoid Structure of CoFeSP. Biochemistry, 2012, 51, 7040-7042.	2.5	14
275	Concepts in bio-molecular spectroscopy: vibrational case studies on metalloenzymes. Physical Chemistry Chemical Physics, 2015, 17, 18222-18237.	2.8	14
276	Distinct chromophore–protein environments enable asymmetric activation of a bacteriophytochrome-activated diguanylate cyclase. Journal of Biological Chemistry, 2020, 295, 539-551.	3.4	14
277	Intramolecular Proton Transfer Controls Protein Structural Changes in Phytochrome. Biochemistry, 2020, 59, 1023-1037.	2.5	14
278	SERR Spectroelectrochemical Study of Cytochrome cd1 Nitrite Reductase Co-Immobilized with Physiological Redox Partner Cytochrome c552 on Biocompatible Metal Electrodes. PLoS ONE, 2015, 10, e0129940.	2.5	14
279	Integration of metallic endoprotheses in dog femur studied by near-infrared Fourier-transform Raman microscopy. Biomaterials, 2002, 23, 1337-1345.	11.4	13
280	Resonance Raman study of the superoxide reductase from Archaeoglobus fulgidus, E12 mutants and a â€~natural variant'. Physical Chemistry Chemical Physics, 2009, 11, 1809.	2.8	13
281	Catalytic efficiency of dehaloperoxidase A is controlled by electrostatics – application of the vibrational Stark effect to understand enzyme kinetics. Biochemical and Biophysical Research Communications, 2013, 430, 1011-1015.	2.1	13
282	Substrate–Protein Interactions of Type II NADH:Quinone Oxidoreductase from <i>Escherichia coli</i> . Biochemistry, 2016, 55, 2722-2734.	2.5	13
283	Influence of Mesityl and Thiophene Peripheral Substituents on Surface Attachment, Redox Chemistry, and ORR Activity of Molecular Iron Porphyrin Catalysts on Electrodes. Inorganic Chemistry, 2019, 58, 10637-10647.	4.0	13
284	Role of the Propionic Side Chains for the Photoconversion of Bacterial Phytochromes. Biochemistry, 2019, 58, 3504-3519.	2.5	13
285	<i>In Vitro</i> Assembly as a Tool to Investigate Catalytic Intermediates of [NiFe]-Hydrogenase. ACS Catalysis, 2020, 10, 13890-13894.	11.2	13
286	Generation of a μ-1,2-hydroperoxo FellIFellI and a μ-1,2-peroxo FelVFellI Complex. Nature Communications, 2022, 13, 1376.	12.8	13
287	Structural studies of yeast Iso-1 cytochrome c mutants by resonance Raman spectroscopy. FEBS Journal, 1991, 201, 211-216.	0.2	12
288	Vibrational analysis of biliverdin IXα dimethyl ester conformers. Journal of Molecular Structure, 1995, 348, 225-228.	3.6	12

#	Article	IF	CITATIONS
289	Vibrational spectroscopy of hypericin, its sodium salt and pyridinium complex. Journal of Molecular Structure, 1997, 407, 5-10.	3.6	12
290	Electric-Field Dependent Decays of Two Spectroscopically Different M-States of Photosensory Rhodopsin II from Natronobacterium pharaonis. Biophysical Journal, 2003, 84, 3864-3873.	0.5	12
291	Surface-Enhanced Vibrational Spectroelectrochemistry: Electric-Field Effects on Redox and Redox-Coupled Processes of Heme Proteins. , 2006, , 313-334.		12
292	Nature of the Surface-Exposed Cytochrome–Electrode Interactions in Electroactive Biofilms of <i>Desulfuromonas acetoxidans</i> . Journal of Physical Chemistry B, 2015, 119, 7968-7974.	2.6	12
293	Surface enhanced resonance Raman detection of a catalytic intermediate of DyP-type peroxidase. Physical Chemistry Chemical Physics, 2015, 17, 11954-11957.	2.8	12
294	Ultrafast proton-coupled isomerization in the phototransformation of phytochrome. Nature Chemistry, 2022, 14, 823-830.	13.6	12
295	Electron transfer between cytochrome c and microsomal monooxygenase generates reactive oxygen species that accelerates apoptosis. Redox Biology, 2022, 53, 102340.	9.0	12
296	Resonance Raman spectroscopic study of the tryptic 39-kDa fragment of phytochrome. FEBS Letters, 2000, 482, 252-256.	2.8	11
297	An expanded genetic code for probing the role of electrostatics in enzyme catalysis by vibrational Stark spectroscopy. Biochimica Et Biophysica Acta - General Subjects, 2017, 1861, 3053-3059.	2.4	11
298	Characterization of anisotropically shaped silver nanoparticle arrays via spectroscopic ellipsometry supported by numerical optical modeling. Applied Surface Science, 2017, 421, 460-464.	6.1	11
299	Electrochemical and Resonance Raman Spectroscopic Studies of Waterâ€Oxidizing Ruthenium Terpyridyl–Bipyridyl Complexes. ChemSusChem, 2017, 10, 551-561.	6.8	11
300	Spectroscopic, thermodynamic and computational evidence of the locations of the FADs in the nitrogen fixation-associated electron transfer flavoprotein. Chemical Science, 2019, 10, 7762-7772.	7.4	11
301	A bioinspired oxoiron(<scp>iv</scp>) motif supported on a N ₂ S ₂ macrocyclic ligand. Chemical Communications, 2021, 57, 2947-2950.	4.1	11
302	Molecule-specificity of surface enhanced Raman scattering. Journal of Molecular Structure, 1995, 349, 137-140.	3.6	10
303	Resonance Raman Spectroscopy of the Integral Quinol Oxidase Complex ofSulfolobus acidocaldariusâ€. Biochemistry, 1996, 35, 12796-12803.	2.5	10
304	Active site structure and dynamics of cytochromec3 fromDesulfovibrio gigas immobilized on electrodes. Biopolymers, 2002, 67, 331-334.	2.4	10
305	Impact of Amino Acid Substitutions near the Catalytic Site on the Spectral Properties of an O ₂ â€Tolerant Membraneâ€Bound [NiFe] Hydrogenase. ChemPhysChem, 2010, 11, 1215-1224.	2.1	10
306	Copper Complexes of "Superpodal―Amine Ligands and Reactivity Studies towards Dioxygen. European Journal of Inorganic Chemistry, 2012, 2012, 3000-3013.	2.0	10

#	Article	IF	CITATIONS
307	Reductive activation and structural rearrangement in superoxide reductase: a combined infrared spectroscopic and computational study. Physical Chemistry Chemical Physics, 2014, 16, 14220-14230.	2.8	10
308	Metal-induced histidine deprotonation in biocatalysis? Experimental and theoretical insights into superoxide reductase. RSC Advances, 2014, 4, 54091-54095.	3.6	10
309	Changing the chemical and physical properties of high valent heterobimetallic bis-(μ-oxido) Cu–Ni complexes by ligand effects. Dalton Transactions, 2016, 45, 15994-16000.	3.3	10
310	Carbon Monoxide Dehydrogenase Reduces Cyanate to Cyanide. Angewandte Chemie - International Edition, 2017, 56, 7398-7401.	13.8	10
311	The Lumi-R Intermediates of Prototypical Phytochromes. Journal of Physical Chemistry B, 2020, 124, 4044-4055.	2.6	10
312	A Resonance Raman Marker Band Characterizes the Slow and Fast Form of Cytochrome c Oxidase. Journal of the American Chemical Society, 2021, 143, 2769-2776.	13.7	10
313	Local Electric Field Changes during the Photoconversion of the Bathy Phytochrome Agp2. Biochemistry, 2021, 60, 2967-2977.	2.5	10
314	Distance-dependent electron transfer rate of immobilized redox proteins: A statistical physics approach. Physical Review E, 2010, 81, 046101.	2.1	9
315	On the pH-Modulated Ru-Based Prodrug Activation Mechanism. Inorganic Chemistry, 2019, 58, 1216-1223.	4.0	9
316	Structural changes in cytochrome c oxidase induced by cytochrome c binding. A resonance Raman study. BBA - Proteins and Proteomics, 2000, 1480, 57-64.	2.1	8
317	Excited state geometry calculations and the resonance Raman spectrum of hexamethylpyrromethene. Journal of Molecular Structure, 2003, 661-662, 611-624.	3.6	8
318	Combining Spectroscopy and Theory to Evaluate Structural Models of Metalloenzymes: A Case Study on the Soluble [NiFe] Hydrogenase from <i>Ralstonia eutropha</i> . ChemPhysChem, 2013, 14, 185-191.	2.1	8
319	Dual-wavelength photoacoustic imaging of a photoswitchable reporter protein. Proceedings of SPIE, 2016, , .	0.8	8
320	Switchable Redox Chemistry of the Hexameric Tyrosine-Coordinated Heme Protein. Journal of Physical Chemistry B, 2017, 121, 3955-3964.	2.6	8
321	A New Domain of Reactivity for Highâ€Valent Dinuclear [M(μâ€O) 2 M′] Complexes in Oxidation Reactions. Angewandte Chemie, 2017, 129, 303-307.	2.0	8
322	Light- and temperature-dependent dynamics of chromophore and protein structural changes in bathy phytochrome Agp2. Physical Chemistry Chemical Physics, 2021, 23, 18197-18205.	2.8	8
323	On the Role of the Conserved Histidine at the Chromophore Isomerization Site in Phytochromes. Journal of Physical Chemistry B, 2021, 125, 13696-13709.	2.6	8
324	Resonance Raman study of the cytochrome P-450 LM2-halothane intermediate complex. FEBS Letters, 1988, 237, 15-20.	2.8	7

#	Article	IF	CITATIONS
325	Time-Resolved and Two-Dimensional NIR FT-Raman Spectroscopy. Applied Spectroscopy, 1993, 47, 1452-1456.	2.2	7
326	Raman Spectroscopic Study of the Blue Copper Protein Halocyanin from Natronobacterium pharaonis. Biochemistry, 1994, 33, 11426-11431.	2.5	7
327	<title>Medical diagnostics with NIR-FT-Raman spectroscopy</title> ., 1998, , .		7
328	Structural and spectroscopic characterization of ClC(O)SNSO. A theoretical and experimental study. Physical Chemistry Chemical Physics, 1999, 1, 2551-2557.	2.8	7
329	Time-resolved methods in Biophysics. 1. A novel pump and probe surface-enhanced resonance Raman approach for studying biological photoreceptors. Photochemical and Photobiological Sciences, 2006, 5, 1103.	2.9	7
330	Structural communication between the chromophoreâ€binding pocket and the Nâ€ŧerminal extension in plant phytochrome phyB. FEBS Letters, 2017, 591, 1258-1265.	2.8	7
331	Spectroelectrochemical insights into structural and redox properties of immobilized endonuclease III and its catalytically inactive mutant. Spectrochimica Acta - Part A: Molecular and Biomolecular Spectroscopy, 2018, 188, 149-154.	3.9	7
332	Ultraviolet resonance Raman enhancement of the carboxylate and guanidinium groups in amino acids. Journal of Raman Spectroscopy, 1989, 20, 645-650.	2.5	6
333	Structural studies of cytochrome c-554 from Chloroflexus aurantiacus by resonance Raman spectroscopic techniques. Biochimica Et Biophysica Acta - Bioenergetics, 1991, 1060, 196-202.	1.0	6
334	More than fine tuning. Science, 2014, 346, 1456-1457.	12.6	6
335	Accelerated Photoâ€Induced Degradation of Benzidine―p â€Aminothiophenolate Immobilized at Lightâ€Enhancing TiO 2 Nanotube Electrodes. Chemistry - A European Journal, 2019, 25, 16048-16053.	3.3	6
336	Photoreactions of the Histidine Kinase Rhodopsin Ot-HKR from the Marine Picoalga Ostreococcus tauri. Biochemistry, 2019, 58, 1878-1891.	2.5	6
337	Stable, but still reactive – investigations on the effects of Lewis acid binding on copper nitrene intermediates. Zeitschrift Fur Anorganische Und Allgemeine Chemie, 2021, 647, 1495-1502.	1.2	6
338	Photoinduced reaction mechanisms in prototypical and bathy phytochromes. Physical Chemistry Chemical Physics, 2022, 24, 11967-11978.	2.8	6
339	The effect of pH and hydrogen-deuterium exchange on the heme pocket structure of cytochrome c probed by resonance Raman spectroscopy. Journal of Molecular Structure, 1995, 349, 125-128.	3.6	5
340	Surface-enhanced resonance Raman study of cytochrome c″ from Methylophilus Methylotrophus. Journal of Molecular Structure, 2001, 565-566, 193-196.	3.6	5
341	Resonance Raman Spectroscopy for In-Situ Monitoring of Radiation Damage. AIP Conference Proceedings, 2007, , .	0.4	5
342	Domain motions and electron transfer dynamics in 2Fe-superoxide reductase. Physical Chemistry Chemical Physics, 2016, 18, 23053-23066.	2.8	5

#	Article	IF	CITATIONS
343	Resonance Raman spectroscopic analysis of the iron–sulfur cluster redox chain of the Ralstonia eutropha membraneâ€bound [NiFe]â€hydrogenase. Journal of Raman Spectroscopy, 0, , .	2.5	4
344	Resonance raman spectroscopic study of the terminal oxidase complex of Sulfolobus acidocalcdarius. Journal of Inorganic Biochemistry, 1995, 59, 283.	3.5	3
345	Biochemical Applications of Raman Spectroscopy. , 1999, , 88-97.		3
346	Induction of photochemical auto-reduction of cytochrome-c oxidase by an organic peroxide. Biochimica Et Biophysica Acta - Bioenergetics, 2000, 1459, 125-130.	1.0	3
347	Plasmonic Cu/CuCl/Cu ₂ S/Ag and Cu/CuCl/Cu ₂ S/Au Supports with Peroxidase-Like Activity: Insights from Surface Enhanced Raman Spectroscopy. Zeitschrift Fur Physikalische Chemie, 2018, 232, 1541-1550.	2.8	3
348	Quantification of Hv1-induced proton translocation by a lipid-coupled Oregon Green 488-based assay. Analytical and Bioanalytical Chemistry, 2018, 410, 6497-6505.	3.7	3
349	A Pseudotetrahedral Terminal Oxoiron(IV) Complex: Mechanistic Promiscuity in Câ^'H Bond Oxidation Reactions. Angewandte Chemie, 2021, 133, 6826-6830.	2.0	3
350	Structural Changes of Cytochrome c552 from Thermus thermophilus Adsorbed on Anionic and Hydrophobic Surfaces Probed by FTIR and 2D-FTIR Spectroscopy. ChemBioChem, 2001, 2, 180-189.	2.6	3
351	Redox Equilibria of Cytochrome C3 Immobilised on Self-Assembled Monolayers Coated Silver Electrodes. Physica Scripta, 2005, , 225.	2.5	2
352	The influence of secondary interactions on the [Ni(O2)]+ mediated aldehyde oxidation reactions. Journal of Inorganic Biochemistry, 2021, 227, 111668.	3.5	2
353	Electron-Transfer Processes of Cytochrome c at Interfaces. New Insights by Surface-Enhanced Resonance Raman Spectroscopy. ChemInform, 2005, 36, no.	0.0	1
354	Heme Proteins. , 0, , 227-282.		1
355	Adhesion-Induced Domain Formation in Multicomponent Membranes. Biophysical Journal, 2014, 106, 287a.	0.5	1
356	Ein Sâ€oxygenierter [NiFe]â€Komplex als Modell für Sulfenat―intermediate einer O ₂ â€ŧoleranter Hydrogenase. Angewandte Chemie, 2017, 129, 2243-2247.	¹ 2.0	1
357	Catalytic dioxygen reduction mediated by a tetranuclear cobalt complex supported on a stannoxane core. Dalton Transactions, 2020, 49, 6065-6073.	3.3	1
358	Molecular Details on Multiple Cofactor Containing Redox Metalloproteins Revealed by Infrared and Resonance Raman Spectroscopies. Molecules, 2021, 26, 4852.	3.8	1
359	Fourier transform nearâ€infrared resonance Raman spectroscopic study of the α-subunit of phycoerythrocyanin and phycocyanin from the cyanobacterium Mastigocladus laminosus. Journal of Raman Spectroscopy, 1998, 29, 939-944.	2.5	1
360	Cytochrome c at charged interfaces studied by resonance Raman and surface-enhanced resonance Raman spectroscopy. , 1991, , .		0

#	Article	IF	CITATIONS
361	Structures, energies and vibrational spectra of oligopyrroles. Models of the chromophore of phytochrome. AIP Conference Proceedings, 1995, , .	0.4	0
362	Biochemical Applications of Raman Spectroscopy*. , 1999, , 118-127.		0
363	Calculation of the Resonance Raman Intensities of Nickel bis-Dimethylglyoxime by means of Density Functional Theory and the Transform Theory. Journal of Computational Methods in Sciences and Engineering, 2002, 2, 405-410.	0.2	0
364	Copper incorporation into recombinant CotA-laccase from Bacillus subtilis: Characterization of fully copper loaded enzymes. Journal of Biotechnology, 2008, 136, S320.	3.8	0
365	Protein-Cofactor Interactions in Biological Processes. ChemPhysChem, 2010, 11, 1075-1076.	2.1	0
366	Immobilized Redox Proteins: Mimicking Basic Features of Physiological Membranes and Interfaces. , 0, , \cdot		0
367	A Combined SERR Spectroscopic And Electrochemical Approach To Study Enzymes On Electrodes. , 2010, , .		0
368	Disentangling Interactions of an Azole Antibiotic with a Flavohemoglobin from S. aureus. , 2010, , .		0
369	Induced SER Activity Of Au, Pt And TiO[sub 2] Films In Ag Hybrid Devices Via Long Range Plasmon Coupling. , 2010, , .		0
370	Induced SER Activity in Ag-Pt Hybrid Devices. , 2010, , .		0
371	Die Kohlenmonoxidâ€Dehydrogenase reduziert Cyanat zu Cyanid. Angewandte Chemie, 2017, 129, 7504-7507.	2.0	0
372	Raman Spectroscopy, Biochemical Applications. , 2017, , 906-914.		0
373	Surface-Enhanced Resonance Raman Spectroscopy in Electron Transfer Studies. , 2018, , 1-8.		0
374	Spektroskopische Charakterisierung eines reaktiven [Cu 2 (μâ€OH) 2] 2+ Intermediates in Cu/TEMPOâ€katalysierten aeroben Alkoholoxidationen. Angewandte Chemie, 2021, 133, 23201.	2.0	0
375	Resonance Raman Study on the Role of Water in Bacteriorhodopsin. Springer Proceedings in Physics, 1985, , 246-249.	0.2	0
376	Kinetic Studies on Bacteriorhodopsin by Resonance Raman Spectroscopy. Springer Proceedings in Physics, 1985, , 240-245.	0.2	0
377	Resonance Raman Studies of Bacterial and Mammalian Cytochrome Oxidases. , 1993, , 301-302.		0
378	Resonance Raman Spectroscopy of Phytochrome and Model Compounds. , 1995, , 265-268.		0

Resonance Raman Spectroscopy of Phytochrome and Model Compounds., 1995, , 265-268. 378

#	Article	IF	CITATIONS
379	Resonance Raman Spectroscopic Study of Recombinant Phytochromes. , 1997, , 129-130.		0
380	The Alkaline Conformational Equilibria of Cytochrome C Studied by Resonance Raman Spectroscopy. , 1997, , 87-88.		0
381	Time-Resolved Resonance Raman Spectroscopic Study of the Photocycle of Halorhodopsin. , 1997, , 121-122.		0
382	Vibrational Analysis of Linear Methine-Bridged Tetrapyrroles. , 1997, , 525-526.		0
383	The electron transfer dynamics of cytochrome c 552 from Thermus thermophilus probed by time-resolved surface enhanced resonance Raman spectroscopy. , 1999, , 103-106.		0
384	The mechanism of the electron transfer process from cytochrome c to cytochrome c oxidase studied by resonance Raman spectroscopic techniques. , 1999, , 107-110.		0
385	Binding of cytochrome c to phospholipid vesicles and the perturbation of the liposome and protein structure. , 1999, , 377-378.		0
386	Vibrational analysis of model compounds for the tetrapyrrole chromophore in phytochrome. , 1999, , 171-172.		0
387	Resonance Raman Spectroscopy of Protein–Cofactor Complexes. , 2018, , 1-10.		0
388	Surface-Enhanced Vibrational Spectroelectrochemistry: Electric-Field Effects on Redox and Redox-Coupled Processes ofÂHeme Proteins. , 2006, , 313-334.		0